SDC

QUANTITATIVE ANALYSIS OF STRUCTURAL ALTERATIONS IN THE CHOROID OF PATIENTS WITH ACTIVE BEHÇET UVEITIS

SUMRU ONAL, MD, FEBOPHTH,*† GUNAY ULUDAG, MD,‡ MERIH ORAY, MD,§ EMRE MENGI, PHD,¶ CARL P. HERBORT, MD, FEBOPHTH,**†† MEHMET AKMAN, MD, MPH,‡‡ MUSTAFA M. METIN, MS,§§ AYLIN KOC AKBAY, MD,‡ ILKNUR TUGAL-TUTKUN, MD§

Purpose: To quantitatively analyze in vivo morphology of subfoveal choroid during an acute attack of Behçet uveitis.

Methods: In this prospective study, 28 patients with Behçet uveitis of ≤4-year duration, and 28 control subjects underwent enhanced depth imaging optical coherence tomography. A novel custom software was used to calculate choroidal stroma-to-choroidal vessel lumen ratio. Subfoveal choroidal thickness was measured at fovea and 750 μm nasal, temporal, superior, and inferior to fovea. Patients underwent fluorescein angiography and indocyanine green angiography. Receiver operating characteristic curve and area under the curve were computed for central foveal thickness. The eye with a higher Behçet disease ocular attack score of 24 was studied. The main outcome measures were choroidal stroma-to-choroidal vessel lumen ratio and choroidal thickness.

Results: The mean total Behçet disease ocular attack score of 24, fluorescein angiography, and indocyanine green angiography scores were 7.42 ± 4.10, 17.42 ± 6.03, and 0.66 ± 0.73, respectively. Choroidal stroma-to-choroidal vessel lumen ratio was significantly higher in patients (0.413 ± 0.056 vs. 0.351 ± 0.063, $P = 0.003$). There were no significant differences in subfoveal choroidal thickness between patients and control subjects. Choroidal stroma-to-choroidal vessel lumen ratio correlated with retinal vascular staining and leakage score of fluorescein angiography ($r = 0.300$, $P = 0.036$). Central foveal thickness was significantly increased in patients (352.750 ± 107.134 μm vs. 263.500 ± 20.819 μm, $P < 0.001$). Central foveal thickness showed significant correlations with logarithm of minimum angle of resolution vision, Behçet disease ocular attack score of 24, total fluorescein angiography score, retinal vascular staining and/or leakage and capillary leakage scores of fluorescein angiography, and total indocyanine green angiography score. At 275 μm cutoff, diagnostic sensitivity and specificity of central foveal thickness for acute Behçet uveitis were 89% and 72%, respectively (area under the curve = 0.902; 95% CI = 0.826–0.978, $P < 0.001$).

Conclusion: There was choroidal stromal expansion which was not associated with thickening of the choroid. Central foveal thickness may be used as a noninvasive measure to assess inflammatory activity in early Behçet uveitis.

RETINA 0:1–13, 2017

Ocular involvement of Behçet disease is characterized by bilateral nongranulomatous panuveitis with retinal vasculitis. Diffuse vitritis, occlusive retinal vasculitis, retinal infiltrations, cystoid macular edema, and optic nerve head inflammation are the typical signs of active inflammation in the posterior segment of the eye. Recurrent inflammatory attacks of variable severity involving the posterior segment determine the visual prognosis.[1] Therefore, the activity and severity of ocular involvement and the efficacy of therapy need to be closely monitored. Since retinal vasculature is predominantly involved in Behçet disease, fluorescein angiography (FA) is the gold standard imaging modality to detect and monitor the extent of posterior segment inflammatory activity.[2,3]

As Behçet disease is a systemic vasculitis, it might be expected to lead to primary involvement of the choroid vessels as well. Choroidal inflammation may

also develop secondary to severe retinal inflammation. Choroidal involvement in Behçet uveitis has been implicated based on histopathology, indocyanine green angiography (ICGA), and ophthalmic ultrasonography findings. Histopathologic studies have shown diffuse and focal infiltration of the choroid with lymphocytes and macrophages.[4–6] Presence of hypo- and hyperfluorescent spots, irregular filling of choriocapillaris, choroidal filling defects, staining of and leakage from choroidal vessels, and optic disk and diffuse choroidal hyperfluorescence in the intermediate or late phase of ICGA were reported as ICGA signs suggestive of choroidal involvement in Behçet disease.[7–11] Ophthalmic ultrasonography revealed choroidal thickening in eyes with Behçet uveitis; however, because of its low resolution, ultrasonography lacks detailed information.[12,13] Although these studies suggest choroidal vasculitis, choroidal involvement is not clinically evident in Behçet uveitis.

Enhanced depth imaging optical coherence tomography (EDI OCT), already integrated into most commercially available optical coherence tomography (OCT) machines, provides in vivo, cross-sectional, histologic information of the choroid including choroidal thickness measurements and imaging of choroidal structure.[14] At present, there are four publications reporting on choroidal thickness analysis by EDI OCT in patients with Behçet uveitis.[15–18] Their outcomes are conflicting as three studies report thickening of the choroid[15–17] and one suggests thinning of the choroid in patients with Behçet uveitis.[18] The discrepancies in choroidal thickness are likely because of nonhomogenous patient recruitment in terms of activity, anatomical involvement, and duration of Behçet uveitis.

We herein evaluated in vivo quantitative morphology of subfoveal choroid and choroidal thickness using EDI OCT in patients with an acute attack of Behçet uveitis, and compared with age-, sex-, and spherical equivalent of refractive error-matched healthy subjects. A novel custom software was used to segment the choroidal into stroma and vessel lumen. Furthermore, we assessed the intercorrelations between the EDI OCT choroidal parameters and ICGA and FA findings, visual acuity, clinical composite score of uveitis attack severity, anterior chamber flare, and central foveal thickness (CFT) measurement.

Materials and Methods

This prospective cross-sectional study was approved by the institutional review board of Koc University (approval number: 2014.197.IRB1.011). All patients were white and of Turkish descent. The study was conducted according to the tenets of the Declaration of Helsinki and an informed consent was obtained from the patients.

Patient and Control Subject Recruitment

Twenty-eight consecutive Behçet disease patients who attended two tertiary referral uveitis clinics and deemed to have an acute uveitis attack involving the posterior segment of the eye by two observers (ITT and SO) were included from May 1, 2015 to March 30, 2016. Uveitis attack involving the posterior segment was defined as an increase in or the development of vitreous haze, the emergence of inflammatory sheathing of retinal vessels, vascular occlusion, retinal hemorrhages, retinal infiltrates, macular edema, and/or papillitis.

Exclusion criteria were a duration of Behçet uveitis for more than 4 years, eyes with spherical equivalent refractive error of more than ±5.00 diopters, eyes with visually significant cataract or media opacity obscuring precise visualization of the choroidoscleral interface, eyes with concurrent ocular disease, patients with a comorbidity such as diabetes mellitus, systemic hypertension or other coexistent autoimmune disease, eyes with a history of ocular surgery and/or intravitreal injection/implant, patients with a history of refractive surgery, and patients aged 18 years or younger, and patients aged 50 years or older.

Age-, sex-, and spherical equivalent of refractive error-matched healthy subjects were recruited from consecutive patients who were scheduled for routine

From the *Department of Ophthalmology, School of Medicine, Koc University, Istanbul, Turkey; †Department of Ophthalmology, V.K. Foundation, American Hospital, Istanbul, Turkey; ‡Department of Ophthalmology, Koc University Hospital, Istanbul, Turkey; §Department of Ophthalmology, Istanbul Faculty of Medicine, Istanbul University, Istanbul, Turkey; ¶Department of Mathematics, Koc University, Istanbul, Turkey; **University of Lausanne, Lausanne, Switzerland; ††Retinal and Inflammatory Eye Diseases, Centre for Ophthalmic Specialized Care (COS), Lausanne, Switzerland; ‡‡Department of Family Medicine, School of Medicine, Marmara University, Istanbul, Turkey; and §§School of Medicine, Koc University, Istanbul, Turkey.

This study has been nonfinancially (angiographic dyes and equipment) supported by the Koc University Hospital and the Istanbul University Scientific Projects (project number 25575).

I. Tugal-Tutkun has received financial support outside the submitted work, including honoraria from Servier, AbbVie, Santen, and Allergan. The remaining authors have no conflicting interests to disclose.

Supplemental digital content is available for this article. Direct URL citations appear in the printed text and are provided in the HTML and PDF versions of this article on the journal's Web site (www.retinajournal.com).

Reprint requests: Sumru Onal, MD, FEBOphth, Koc Universitesi Tip Fakultesi Hastanesi, Goz Hastaliklari Davutpasa Cad. No: 4, 34010 Topkapi, Istanbul, Turkey; e-mail: sumruo_md@yahoo.com

ocular examination for refractive error correction at the Koc University Hospital.

Ocular Examination

All patients underwent a complete ophthalmologic examination, including best-corrected visual acuity, slit-lamp biomicroscopy, tonometry, and indirect ophthalmoscopy. A decimal scale Snellen chart and equipment that yielded each patient's best refractive correction were used to determine visual acuity. Visual acuities were converted to logarithm of minimum angle of resolution scale. Laser flare photometer (KOWAFC-2000; KowaCo Ltd, Tokyo, Japan) was used to measure anterior chamber flare in patients seen at the Istanbul Faculty of Medicine.

Uveitis Attack Severity Scoring

The severity of uveitis attack was scored for each eye based on the Behçet disease ocular attack score 24 (BOS24) developed by Kaburaki et al.[19] It consists of a total 24 points summarized from 6 parameters of ocular inflammatory signs, including anterior chamber cells (0–4), vitreous haze (0–4), peripheral fundus lesions (0, 2, 4, 6, 8), posterior pole lesions (0, 2, 3, 4), foveal lesions (0, 2), and optic disk lesions (0, 2).

Scoring of Anterior Chamber Cells and Vitreous Haze

Cells in the anterior chamber are graded from 0 to 4 using a semiquantitative scoring system. Vitreous haze is also graded using a semiquantitative scoring system based on the clarity of the optic disk, retinal vessels, and nerve fiber layers, and is graded from 0 to 4. Both anterior chamber cells and vitreous haze grades are based on the standardization of uveitis nomenclature working group grading.[20]

Scoring of Retinal Inflammatory Signs

The retina is divided into peripheral retina (areas outside of arcade vessels) and posterior pole (areas inside of arcade vessels). Peripheral retina is further divided into four quadrants by a horizontal and vertical line passing through the fovea. When scoring the peripheral retina, two points are added for each quadrant with new inflammatory signs, that is, any new retinal exudates or hemorrhages. Retinal edema is not scored in the absence of other findings. When scoring the posterior pole of the retina, the percentage of the area of new inflammatory signs (hemorrhages, exudates) occupying areas of the posterior pole is determined. If the percentage of area of new inflammatory signs is less than 10%, 2 points; if the percentage is 10% or more and less than 25%, 3 points; and if the percentage is 25% or more, 4 points are assigned.

Scoring of Foveal and Optic Disk Lesions

For any new hemorrhages or exudates observed in the fovea, two points are added as foveal lesion score. If there are new inflammatory signs of the optic disk (redness and edema, sometimes accompanied by hemorrhages, exudates, retinal edema surrounding the optic disk) two points are added as the optic disk lesion score.

In patients with bilateral activation, the eye with a higher BOS24 score was selected as the study eye; if both eyes had identical BOS24 scores, one eye was randomly assigned for analysis. The eye of control subjects was selected based on the laterality of the study eye of the patients. All imaging procedures described below were done on the same day as the uveitis attack scoring.

Optical Coherence Tomography Scanning Procedures and Subfoveal Choroidal Thickness and Central Foveal Thickness Measurements

Examinations were accomplished by the Heidelberg Spectralis spectral-domain optical coherence tomography device (Heidelberg Engineering, Heidelberg, Germany) with software version 6.0, and after pupillary dilation using tropicamide 1% and phenylephrine hydrochloride 2.5%. To avoid diurnal variations, measurements were performed at around noon. The Spectralis device contains an 870-nm wavelength superluminescent diode laser and is capable of obtaining 40,000 A-scans per second.

Following the guidelines of the Spectralis user manual, the subjects' keratometry readings and the most recent refraction were entered into the software program to estimate optical magnification and, therefore, to allow for more accurate comparisons across individuals. The spherical equivalent of refractive error was calculated as the sphere plus half a cylinder. Results from manifest refraction were used for analysis. Choroidal thickness was defined as the distance from the outer border of the hyperreflective retinal pigment epithelium perpendicular to the choroidoscleral interface.

The built-in EDI OCT feature in the Heidelberg software was used to evaluate the choroid. The scan patterns consisted of 2 single line scans obtained horizontally and vertically, and one cross-hair scan within $5 \times 30°$ of fixation averaged for 100 scans using the automatic averaging and eye-tracking features. One horizontal and one vertical scan with the best image quality (Q-factor) were selected from the

different scan patterns for evaluation. Images with a Q-factor less than 25 were not included for analysis. Images were captured with the high-speed acquisition mode and have a digital resolution of 3.9 μm axially × 11 μm laterally.

Using digital calipers provided by the Heidelberg Spectralis OCT software, choroidal thickness was measured manually at 5 locations: at the fovea and at 750 μm nasal, temporal, superior, and inferior to the fovea. To avoid possible overestimation of choroidal thickness in measurements based on 1:1 pixel image, measurements were performed using 1:1 μm images. Two experienced independent observers (SO, GU) blind to each other's readings measured subfoveal choroidal thicknesses, measurements were averaged for analysis. A magnification of at least 100% to 200% was used to place the measurement line precisely. The observers were also allowed to adjust the contrast of the image to better delineate choroidal boundaries. However, measurements were not taken in eyes or at locations where the posterior border of the choroid was poorly demarcated despite the procedures described above.

One 25-line raster spectral-domain optical coherence tomography image with a scan size of 30 × 25° and automatic real time set at 25 was obtained and CFT was recorded from the central 1 mm Early Treatment Diabetic Retinopathy Study grid display on the thickness map report.

Light-To-Dark (Choroidal Stroma-To-Choroidal Vessel Lumen) Ratio Calculation

A custom software was developed using MATLAB software (The Math Works, Inc, Natick, MA). Optical coherence tomography scans were exported from the OCT acquisition software as grayscale, compression-free, quality-preserving TIFF images. A region of interest of 1.5 mm width centered below the fovea in the choroid was selected manually (Figure 1). Light-to-dark ratio was calculated according to the threshold levels obtained by Otsu's method.[21,22] A separate Otsu threshold was determined for each pixel in the region of interest, locally. The threshold determined for a pixel minimizes the intraclass variances of two classes (comprised of pixels below and above the threshold) in a 21 × 21 pixel rectangular region at the center of which the pixel of interest is located. Within the region of interest, a pixel above its local threshold is designated as a light pixel and corresponds to choroidal stroma, whereas a pixel below its local threshold is designated as dark and corresponds to the choroidal vessel lumen. Hence the light-to-dark ratio represents choroidal stroma-to-choroidal vessel lumen (CS:CVL) ratio and will be referenced as such throughout the rest of this paper.

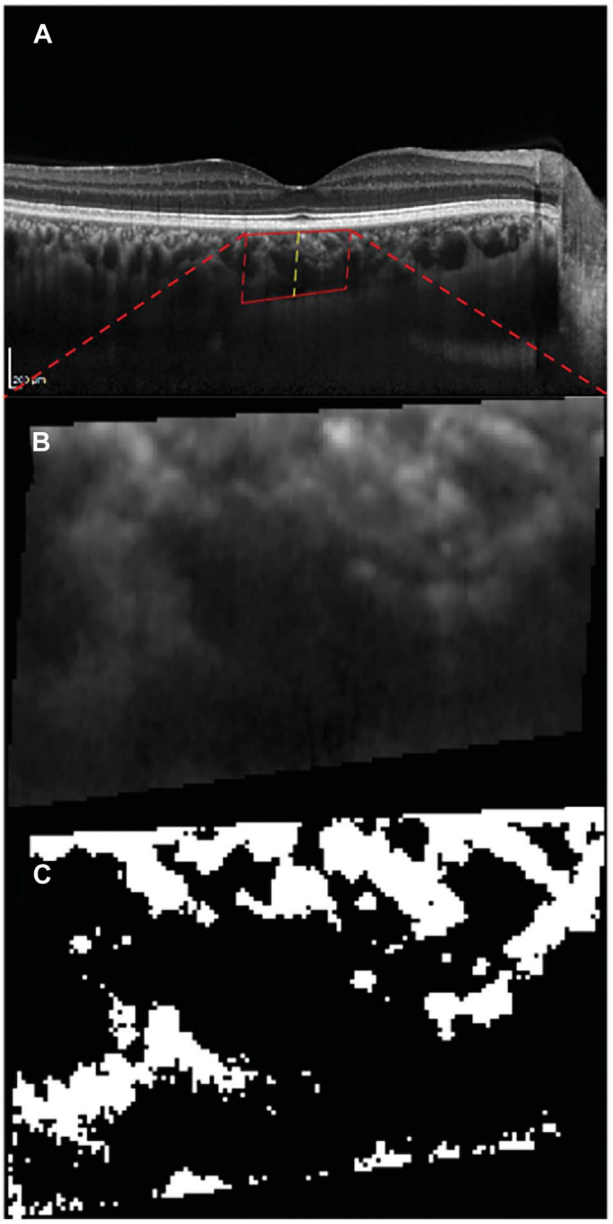

Fig. 1. A. Enhanced depth imaging optical coherence tomography of a healthy eye (Heidelberg Engineering, Heidelberg, Germany). Red box represents selection of subfoveal choroidal region of interest (ROI). **B.** Magnified section of ROI. **C.** ROI after software analysis. White area (light pixels) represents choroidal stroma and black area (black pixels) represents choroidal vessel lumen.

Images were excluded from analysis, in case the observer decided that there was significant noise that could potentially affect the CS:CVL ratio.

Dual Fluorescein and Indocyanine Green Angiography Scoring

Dual FA and ICGA images were obtained from the posterior pole and eight peripheral sweeps at early (0–5 minutes), intermediate (8–12 minutes), and late

(25–30 minutes) phases using the Heidelberg retinal angiograph 2 (Heidelberg Engineering, Heidelberg, Germany) after an intravenous injection of 2.5 mL of 10% sodium fluorescein (Fluorescite; Alcon, Inc, Fort Worth, TX) and 2.5 mL of 5 mg/mL indocyanine green (ICG-Pulsion 25 mg; PULSION Medical Systems SE, Munich, Germany).

An angiographic scoring system developed by the Angiography Scoring for Uveitis Working Group and with proven interobserver reliability was used for scoring of FA and ICGA.[23–26] All angiograms were scored by one experienced ophthalmologist (CPH) who was blind to the clinical findings of the patients.

The angiographic scoring system used herein is a semiquantitative system.[23] The fundus is divided into four quadrants by a horizontal and a vertical line passing through the optic disk. The area between the temporal vascular arcades is defined as the posterior pole. Fluorescein angiography signs include nine categories. Optic disk hyperfluorescence is graded from 0 (normal) to 3 (1 = partial staining, 2 = diffuse staining, and 3 = leakage with blurring of disk margins and papillary vasculature). Macular edema is graded from 1 (faint hyperfluorescence) to 4 (pooling of dye in cystic spaces). Retinal vascular staining and/or leakage are scored separately according to their location. Retinal vascular staining and/or leakage of posterior pole arcades are scored as focal (score of 1), more extended or multifocal, but limited in area (score of 2), or diffuse (score of 3). Involvement of other parts of the retinal vascular tree is graded only as either absent (score of 0) or present (score of 1). Capillary leakage is scored separately for the posterior pole (excluding perifoveal ring of leakage) and for each quadrant. Capillary leakage of the posterior pole is scored as limited (score of 1) or diffuse (score of 2). For each quadrant, foci of leakage limited in area or intensity is scored as 1, and diffuse leakage is scored as 2. Retinal capillary nonperfusion is graded according to the number of quadrants in which it is present. Any area of capillary nonperfusion in the macula (enlargement of foveal avascular zone), posterior pole (excluding macular ischemia), and in each quadrant is given an additional score of 1. Neovascularization of disk is assigned a score of 2. Neovascularization elsewhere is graded with a score of 1 for neovascularization elsewhere at one focus and with a score of 2 for multiple foci. Pinpoint leak is graded as localized if present in three or less disk diameters (score of 1), or extensive if present in more than three disk diameters (score of 2). Retinal staining and/or subretinal pooling are graded as localized if present in three or less disk diameters (score of 1), or extensive if present in more than three disk diameters (score of 4). The maximum score for each angiographic sign is 3 for optic disk hyperfluorescence, 4 for macular edema and retinal staining/subretinal pooling, 7 for retinal vascular staining/leakage, 10 for capillary leakage, 6 for retinal capillary nonperfusion, and 2 for neovascularization of disk, neovascularization elsewhere, and pinpoint leaks. Hence, the total maximum score for a given eye might be 40. Total FA score, retinal vascular staining and/or leakage score, and capillary leakage score were used for correlation analyses in this study.

Based on the angiographic scoring system, ICGA signs include four categories.[23] Early stromal vessel hyperfluorescence is graded separately for the posterior pole and retinal quadrants. A score of 1 is given if it is present in the posterior pole. It is scored as 1 if it is present in one to two quadrants, and as 2 if it is present in more than two quadrants. Choroidal vasculitis (fuzzy choroidal vessels) is categorized as faint (course recognizable, score of 1); as moderate (vessels more blurred but course recognizable) which is further graded as localized/limited if it encompasses one to two quadrants (score of 2), and as diffuse if it encompasses more than two quadrants (score of 3); and as fuzzy vessels without recognizable course, and is graded as localized/limited if it encompasses one to two quadrants (score of 4), and as diffuse if it encompasses more than two quadrants (score of 6). Dark dots/areas (excluding atrophy) are graded separately according to their location. Dark dots/areas of posterior pole are graded as sparse and/or faint (score of 1) or as numerous and/or pronounced (score of 2). Involvement for each quadrant is graded as sparse and/or faint (score of 1), or as numerous and/or pronounced (score of 1.5). Optic disk hyperfluorescence is graded as perceptible (score of 1) or as pronounced (score of 3). The maximum score for each angiographic sign is 3 for early stromal vessel and optic disk hyperfluorescence, 6 for choroidal vasculitis, and 8 for dark dots. The total maximum ICGA score might be 20 for a given eye. Total ICGA score was used for correlation analyses.

Statistical Analysis

Statistical evaluation SPSS 21.0 software was used for statistical analysis (SPSS Inc, Chicago, IL). Interobserver agreement was calculated using intraclass correlation coefficient and 95% confidence intervals. For group comparisons Mann–Whitney *U* test was used. Association of ocular clinical parameters was assessed using Spearman's coefficient of correlation. A correlation coefficient of 0.1 to 0.3 was considered as weak correlation, 0.4 to 0.6 as moderate correlation, 0.7 to 0.9 as strong correlation, and 1.0 of perfect correlation as suggested by Dancey and Reidy.[27]

Table 1. Demographic and Clinical Characteristics of 28 Patients (28 Eyes) With Active Behçet Uveitis and Healthy Control Subjects

Parameter	Behçet Uveitis Mean ± SD Median (Range)	Healthy Control Subjects Mean ± SD Median (Range)	*P*
Gender: male/female	19/9	19/9	—
Age, years n = 28	29.75 ± 7.31 28 (18–46)	30.07 ± 6.94 29 (19–46)	0.812
SE refractive error, D n = 28	−0.22 ± 1.00 0 (−4.25 to 1.00)	−0.46 ± 1.05 −0.25 (−4.50 to 0.75)	0.257
LogMAR visual acuity n = 28	0.28 ± 0.47 (20/38) 0.10 (20/25), (HM–0) (20/40,000–20/20)	0.0 ± 0.0 (20/20) 0.0 (0.0–0.0)	<0.001
AC Flare, ph/ms n = 22	8.66 ± 5.72 8.35 (2.20–25.40)	—	—
Behçet uveitis duration, months n = 28	22.16 ± 20.52 18 (1–48)	—	—
Attack duration, days n = 28	7.29 ± 5.39 7 (1–15)	—	—

AC, anterior chamber; HM, hand motion; logMAR, logarithm of the minimum angle of resolution; SE, spherical equivalent.

Diagnostic sensitivity and specificity and cutoff values were determined using a receiver operating characteristic curve and area under the receiver operating characteristic curve (AUC) analysis. The receiver operating characteristic curve is a useful method to represent the ability of tests or parameters to differentiate between normal and pathologic subjects. In a receiver operating characteristic curve, the true-positive rate (sensitivity) is designed as a function of the false-positive rate (1—specificity) for different cutoff points of a parameter. The resulting AUC indicates how well a parameter can distinguish between the examined groups: control or diseased. The interpretation for AUC is as follows: no discrimination if AUC is ≤ 0.5, acceptable discrimination if AUC is ≥ 0.7 to 0.8, excellent discrimination if AUC is ≥ 0.8 to 0.9, and outstanding discrimination if AUC is ≥ 0.9.[28] A *P* value less than 0.05 was considered statistically significant.

Table 2. BOS24, FA, and ICGA Total and Sign Scores of 28 Eyes of 28 Patients With Active Behçet Uveitis

	Mean ± SD	Median (Range)
BOS24		
Total score	7.42 ± 4.10	6.5 (2–18)
Anterior chamber cells	0.89 ± 1.13	1 (0–4)
Vitreous haze	0.57 ± 0.50	1 (0–1)
Peripheral retinal lesions	3.14 ± 2.51	3 (0–8)
Posterior pole lesions	0.75 ± 1.04	0 (0–3)
Foveal lesions	0.21 ± 0.62	0 (0–2)
Optic disk lesions	1.85 ± 0.52	2 (0–2)
FA		
Total score	17.42 ± 6.03	18 (3–27)
Optic disk hyperfluorescence (5–10 minutes)	2.25 ± 0.75	2 (1–3)
Macular edema (at 10 minutes)	1.61 ± 1.26	1 (0–4)
Retinal vascular staining/leakage (5–10 minutes)	4.14 ± 1.86	5 (0–7)
Capillary leakage (5–10 minutes)	7.78 ± 2.88	9 (0–10)
Retinal capillary nonperfusion	0.39 ± 0.78	0 (0–3)
Neovascularization of the disk	0.14 ± 0.52	0 (0–2)
Neovascularization elsewhere	0.07 ± 0.26	0 (0–1)
Retinal staining (5–10 minutes)	1.14 ± 1.64	0 (0–4)
ICGA		
Total score	0.66 ± 0.73	1 (0–2)
Early stromal vessel hyperfluorescence (0–5 minutes)	0.03 ± 0.19	0 (0–1)
Choroidal vasculitis (10–20 minutes)	0.37 ± 0.49	0 (0–1)
Dark dots or areas excluding atrophy	0.18 ± 0.55	0 (0–2)
Optic disk hyperfluorescence (>15 minutes)	0.05 ± 0.26	0 (0–1)

Results

All patients had bilateral active disease. Twenty-eight eyes of 28 patients (mean age, 29.75 ± 7.31 years; mean spherical equivalent, −0.22 ± 1.00 diopters) with an acute attack of Behçet uveitis were included in the study. Table 1 shows demographic features, refractive error, and logarithm of minimum angle of resolution visual acuity in the patient and control groups; as well as anterior chamber flare values, disease duration, and attack duration in the patient group. There were no significant differences in gender, age, and spherical equivalent of refractive error between the two groups. The duration of Behçet uveitis was 4 years or less in all patients. The median Behçet uveitis duration was 18 months (range: 1–48 months). Median interval between onset of symptoms of a uveitis attack and enrollment was 7 days (range: 1–15 days).

The BOS24, FA, and ICGA scores of 28 eyes with active Behçet uveitis are shown in Table 2. Mean total BOS24, FA, and ICGA scores were 7.42 ± 4.10 (range: 2–18), 17.42 ± 6.03 (range: 3–27), and 0.66 ± 0.73 (range: 0–2), respectively. Total ICGA scores were generally very low and 13 eyes (46.4%) had a total score of zero. The median total FA score was 14 (range: 3–25) in these 13 eyes.

Table 3 shows OCT measurements including CS:CVL ratio, subfoveal choroidal thickness, and CFT in patients and controls. The CS:CVL ratio was significantly higher in eyes with active Behçet uveitis (0.413 ± 0.056) indicating choroidal stromal expansion when compared with the control group (0.351 ± 0.063), (P = 0.003). There were no significant differences between patients with active Behçet uveitis and control subjects in subfoveal choroidal thickness measurements. A good interobserver agreement on subfoveal choroidal thickness measurements was obtained, intraclass correlation coefficients and 95% confidence intervals for 5 subfoveal measurement locations are shown in Table 3. There was a significant increase in CFT in eyes with Behçet uveitis indicating macular edema during the acute attack (352.750 ± 107.134 μm vs. 263.500 ± 20.819 μm, $P < 0.001$). We also calculated study parameters in fellow eyes of patients with active Behçet uveitis (see Table, Supplemental Digital Content 1, which shows results in the fellow eyes; http://links.lww.com/IAE/A623). Figure 2 exemplifies imaging and measurements of the study eye in one representative patient.

As shown in Table 4, there were significant correlations between total FA score and logarithm of minimum angle of resolution visual acuity, BOS24 score,

Table 3. Comparison of Choroidal Stroma-To-Choroidal Vessel Lumen Ratio, Subfoveal Choroidal Thickness, and Central Foveal Thickness Measurements Between Eyes With Active Behçet Uveitis and Control Subjects

Parameter	Behçet Uveitis			Control Subjects				Interobserver Correlation
	Mean ± SD	Median (Range)	n	Mean ± SD	Median (Range)	n	P	ICC (95% CI)
Choroidal stroma-to-choroidal vessel lumen ratio	0.413 ± 0.056	0.409 (0.304–0.510)	24	0.351 ± 0.063	0.346 (0.198–0.444)	28	**0.003**	—
Choroid thickness, μm								
Subfoveal	393.928 ± 74.211	384 (262–572)	28	394.214 ± 101.247	379 (180–698)	28	0.857	0.994 (0.991–0.997)
750 μm nasal to the fovea	363.851 ± 71.353	357 (232–507)	27	369.035 ± 87.799	373.5 (189–632)	28	0.827	0.995 (0.991–0.997)
750 μm temporal to the fovea	378.407 ± 61.488	366 (294–550)	27	370.964 ± 92.225	369 (143–633)	28	0.781	0.991 (0.984–0.994)
750 μm inferior to the fovea	357.695 ± 58.369	353 (271–490)	23	370.821 ± 78.844	360 (183–567)	28	0.455	0.991 (0.985–0.994)
750 μm superior to the fovea	365 ± 52.429	366 (262–461)	23	378.107 ± 83.650	373 (158–590)	28	0.532	0.992 (0.985–0.995)
Central foveal thickness, μm	352.750 ± 107.134	318 (253–703)	28	263.500 ± 20.819	257 (231–307)	28	**<0.001**	—

CI, confidence interval; ICC, intraclass correlation coefficient.

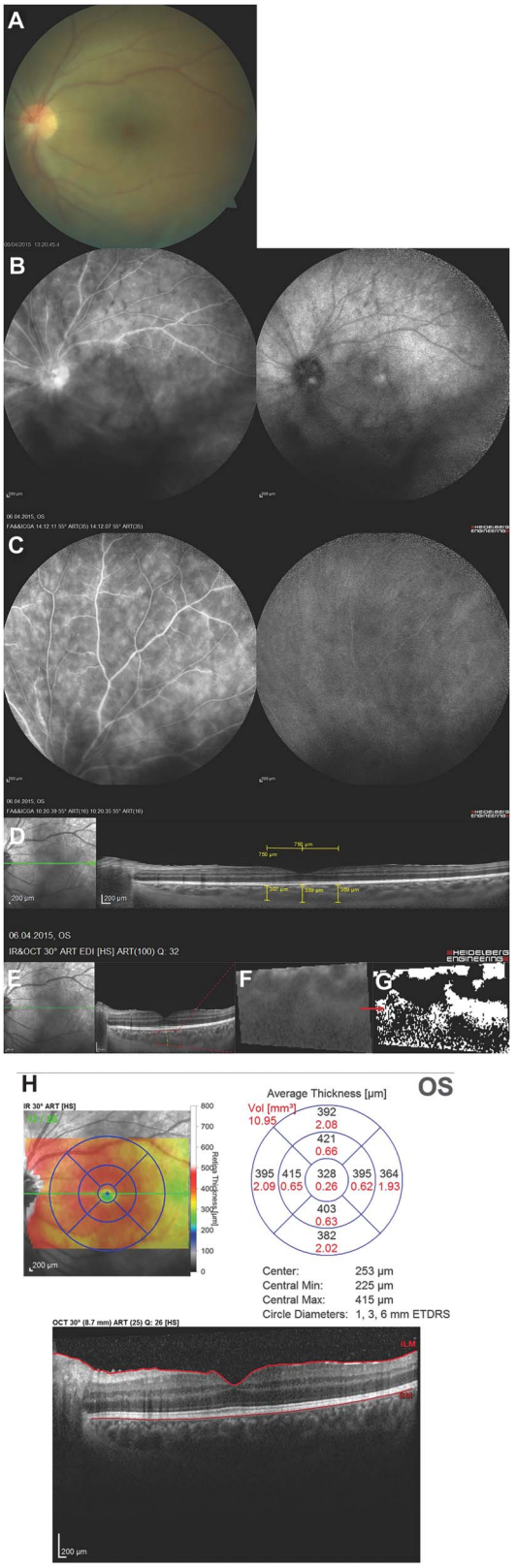

Fig. 2. Imaging and measurements of the study eye in one representative patient. A 25-year-old male patient who had Behçet uveitis for 1 year presented 7 days after onset of ocular symptoms. Posterior segment inflammation was more severe in the left study eye. **A.** Color fundus photograph shows vitreous haze, a small vitreous condensation on the surface of the optic disk, and optic disk hyperemia. Total Behçet disease ocular attack score 24 was calculated as 8 in this eye. **B.** Intermediate phase dual FA and ICGA image obtained from the posterior pole shows focal staining of the optic disk, staining of the superotemporal and nasal retinal vessels on FA, and perceptible optic disk staining on ICGA. Vitreous condensations cause blockage of fluorescence from FA and ICGA. **C.** Intermediate phase dual FA and ICGA frame of superior peripheral retina shows focal retinal vascular staining and diffuse capillary leakage on FA, and faint dark dots on ICGA. Total FA and ICGA scores were 27 and 2, respectively. **D.** Choroidal thicknesses were measured as 359 μm subfoveally, 307 μm 750 μm nasal to the fovea, and 369 μm 750 μm temporal to the fovea on enhanced depth imaging optical coherence tomography obtained as horizontal line scan (Observer 1). **E.** Red box represents the selection of the subfoveal choroidal region of interest (ROI) on enhanced depth imaging optical coherence tomography image. **F.** Magnified section of ROI. **G.** The ROI after software analysis. Choroidal stroma-to-choroidal vessel lumen ratio was 0.382. **H.** Central foveal thickness was recorded as 328 μm from the central 1 mm Early Treatment Diabetic Retinopathy Study grid display on the thickness map report. Optical coherence tomography B-scan shows diffuse macular edema.

anterior chamber flare, total ICGA score and CFT measurements in eyes with active Behçet uveitis. A weak but significant correlation was also observed between the CS:CVL ratio and the retinal vascular staining and/or leakage score of FA ($P = 0.036$). Interestingly, CFT was identified as an imaging parameter exhibiting significant correlations with logarithm of minimum angle of resolution vision, BOS24 score, total FA score, retinal vascular staining and/or leakage and capillary leakage scores of FA, and total ICGA score.

In order to understand the diagnostic value of CFT in predicting the presence of active intraocular inflammation in early Behçet uveitis we calculated a receiver operating characteristic curve (Figure 3). The AUC was 0.902 (95% CI = 0.826–0.978, $P < 0.001$). At a cutoff value of 275 μm or greater the diagnostic sensitivity and specificity of CFT for acute Behçet uveitis were 89% and 72%, respectively.

To further understand the relationship of CS:CVL ratio with disease activity we calculated CS:CVL ratio in 9 study eyes of 3 female and 6 male patients who presented for follow-up from October 15 to November 15, 2016 and were identified to have remission of Behçet uveitis following initiation or augmentation of immunomodulatory therapy. The mean interval between the 2 examinations was 13.88 ± 4.26 months. There was a significant decrease in BOS24 score (6.55 ± 4.58 vs. 0.88 ± 1.05, $P = 0.007$), total FA score (12.55 ± 4.24 vs. 2.55 ± 2.60, $P = 0.008$), and CFT (348.555 ± 141.162 μm vs. 275.666 ± 21.965 μm, $P = 0.028$) during remission of Behçet uveitis. We also observed a decline in CS:CVL ratio (0.432 ± 0.066 vs. 0.383 ± 0.047, $P = 0.161$) during remission, however, it did not reach statistical significance.

Table 4. Intercorrelations Between Clinical Parameters in 56 Eyes of 28 Patients With Active Behçet Uveitis

	LogMAR Visual Acuity		BOS24 Score		AC Flare		Total FA Score		FA: RVS/L		FA: CL		Total ICGA Score		Subfoveal Choroidal Thickness		CS:CVL Ratio	
		P		*P*		*P*		*P*		*P*		*P*		*P*		*P*		*P*
BOS24 score	**0.505***	*<0.001*																
AC flare	**0.396**	*0.008*	**0.528***	*<0.001*														
Total FA score	**0.510***	*<0.001*	**0.426***	*0.001*	**0.394**	*0.008*												
FA: RVS/L	**0.422***	*0.001*	**0.288**	*0.031*	0.266	*0.081*	**0.806***	*<0.001*										
FA: CL	**0.462***	*<0.001*	**0.349**	*0.008*	**0.413***	*0.005*	**0.940***	*<0.001*	**0.745***	*<0.001*								
Total ICGA score	0.114	*0.411*	0.09	*0.52*	0.145	*0.359*	**0.469***	*<0.001*	**0.518***	*<0.001*	**0.491***	*<0.001*						
Subfoveal choroidal thickness	−0.138	*0.313*	0.006	*0.967*	−0.033	*0.835*	−0.221	*0.105*	−0.278	*0.062*	−0.267	*0.080*	0.025	*0.860*				
Choroidal stroma-to-choroidal vessel lumen ratio	0.099	*0.497*	−0.02	*0.891*	0.033	*0.842*	0.187	*0.198*	**0.300**	*0.036*	0.177	*0.225*	0.207	*0.159*	0.251	*0.081*		
Central foveal thickness	**0.586***	*<0.001*	**0.512***	*<0.001*	0.217	*0.156*	**0.605***	*<0.001*	**0.408***	*0.002*	**0.544***	*<0.001*	**0.420***	*0.002*	0.005	*0.97*	0.045	*0.759*

*Correlation coefficient of 0.4 or higher indicating a moderate or stronger correlation.
AC, anterior chamber; CL, capillary leakage; logMAR, logarithm of the minimum angle of resolution; RVS/L, retinal vascular staining/leakage.

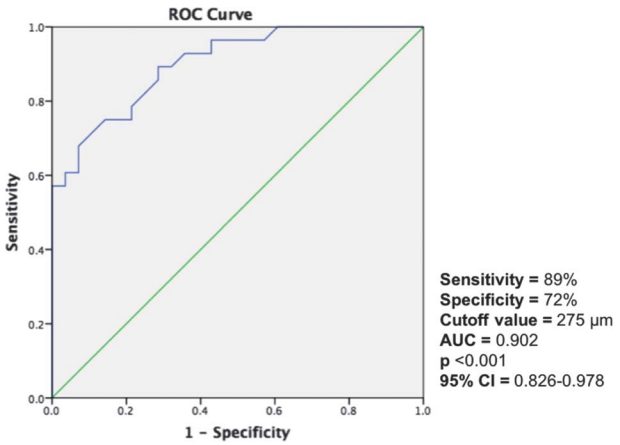

Fig. 3. The receiver operating characteristic curve shows diagnostic value of central foveal thickness in predicting active intraocular inflammation in patients with early Behçet uveitis. CI, confidence interval.

Discussion

This study demonstrated an increased CS:CVL ratio without significant thickening of the choroid in patients with an acute attack of Behçet uveitis at an early stage of the disease. While expansion of the choroidal stroma did not significantly correlate with ICGA and only weakly correlated with vascular staining and/or leakage on FA, CFT on OCT significantly correlated with visual acuity, severity of uveitis attack, FA, and ICGA scores.

Table 5 summarizes comparison of publications reporting on choroidal thickness analysis by EDI OCT in patients with Behçet uveitis and the present study. Two studies reported that subfoveal choroidal thickness was significantly greater during an acute attack of Behçet uveitis than in remission.[15,16] The choroid was also thicker than that of healthy control subjects, not only during an attack of Behçet uveitis, but also during remission of the disease.[16] Another study reported a similar result when they compared eyes in remission of Behçet uveitis with control subjects and found a thicker choroid, although the difference did not reach statistical significance.[17] In contrast, a fourth study demonstrated that the choroid was significantly thinner in eyes of Behçet patients with active posterior uveitis in comparison to control subjects.[18] There was no significant difference in the choroidal thickness between eyes with an acute attack of Behçet uveitis and those in remission.[18] The results of these studies are conflicting because of the nonhomogenous patient populations studied, based on variable definition of activity and remission, anatomical involvement of uveitis, and disease duration. In order to avoid such bias, we included only patients with a duration of Behçet uveitis for 4 years or less, that is, patients with an early disease. It is known that Behçet uveitis is most active during the first 2 to 3 years, and that this period of time is critical for visual prognosis.[29–32] Therefore, we determined a disease duration of ≤4 years as an inclusion criterion. We also recruited only those patients with an acute attack of Behçet uveitis involving the posterior segment of the eye. Our study is not limited to choroidal thickness measurements as previous ones and involves quantitative segmentation of the choroid into choroidal stroma and choroidal vessel lumen through binarization of the EDI OCT images using the Otsu threshold.

Fluorescein angiography and ICGA are both invasive tests that require intravenous administration of dye and imaging up to 10 to 30 minutes.[33–37] In Behçet uveitis, choroidal thickness measured by EDI OCT has been proposed as a noninvasive parameter for assessment of disease activity and the response to therapy.[15,16] Although it is noninvasive, choroidal thickness measurement on EDI OCT imaging has pitfalls. Current software in commercially available OCT devices cannot automatically calculate subfoveal choroidal thickness, manual measurements are tedious and time consuming, and delineating the choroidoscleral interface in subjects with a thick choroid is difficult. As opposed to previous studies, we were not able to demonstrate any significant thickening or thinning of the choroid during an acute attack of Behçet uveitis in patients at an early stage of the disease. However, we observed a significant correlation between CFT and visual acuity, uveitis attack severity score (BOS24 score), total FA score, and FA signs assessing retinal vascular leakage and total ICGA score. Area under the receiver operating characteristic curve for CFT was calculated as 0.902 indicating outstanding discrimination. At a cutoff value of 275 μm diagnostic sensitivity and specificity of CFT for acute Behçet uveitis were 89% and 72%, respectively. Therefore, we propose CFT, an automatically calculated parameter, but not choroidal thickness measurement on EDI OCT, for noninvasive monitoring of inflammatory activity in early Behçet uveitis. In patients with advanced disease and diffuse macular atrophy, CFT may not be a useful measure of inflammatory activity, but could serve as a measure of damage. Takeuchi et al have reported a significant correlation between duration of Behçet uveitis and retinal thinning at the fovea.[38]

Despite the presence of a significant correlation between the total FA score and FA subscores assessing retinal vascular leakage and the total ICGA score, ICGA was not able to show any significant inflammatory activity in the choroid as the median total score was 1 and maximum score was 2 (on a 0–20 scale). In

Table 5. Comparison of Publications Reporting on Choroidal Thickness Analysis by Enhanced Depth Imaging Optical Coherence Tomography in Patients With Behçet Uveitis and the Present Study

Study	Patients (Eyes)	Age (Years), Mean ± SD (Range)	Anatomical Involvement and Activity in Eyes With Behçet Uveitis	Duration (Years), Mean ± SD (Range)	
				Behçet Disease	Uveitis
Ishikawa et al[15]	13 (23)	39.1 ± 11.7 (28–71)	Active posterior uveitis	—	—
Kim et al[16]	30 (30)	47.03 ± 11.01	Active posterior uveitis	—	6.43 ± 3.27
Atas et al[17]	40 (40)	35.95 ± 7.82	20 posterior uveitis, 20 anterior uveitis, all inactive	6.59 ± 3.68 (1–20)	—
Coskun et al[18]	35 (35)	31.5 ± 8.4	26 active posterior uveitis, 9 posterior uveitis in remission	4.1 ± 2.5	—
Present study	28 (28)	29.75 ± 7.31 (18–46)	Active panuveitis	—	22.16 ± 20.52 month (1–48 month)

Study	Subfoveal Choroidal Thickness (μm), Mean ± SD (Range)			Parameter Significantly Correlating With SFCT
	(1) Acute attack	(2) Remission	(3) Control	
Ishikawa et al[15]	337.7 ± 94.5	266.8 ± 89.0	—	Inflammation scores
Kim et al[16]	398.77 ± 155.59	356.72 ± 141.09	259.96 ± 65.16	FA
Atas et al[17]	—	347.23 ± 68	325.92 ± 60.03	None
Coskun et al[18]	291 ± 64	284 ± 103	329 ± 64	Not studied
Present study	393.928 ± 74.211 (262–572)	—	394.214 ± 101.247 (180–698)	None

Ishikawa et al[15]: 1 versus 2, $P < 0.05$; Kim et al[16]: 1 versus 2, $P = 0.004$; 1 versus 3, $P < 0.0001$; 2 versus 3, $P < 0.0001$; Atas et al[17]: 2 versus 3, $P = 0.146$; Coskun et al[18]: 1 versus 2, $P = 0.81$; 1 versus 3, P 0.026; Present study: 1 versus 3, $P = 0.857$.
mo, month(s); SCFT, subfoveal choroidal thickness.

fact, 46.4% of eyes had a total score of zero on ICGA in our study, while FA showed scores up to 25 in these eyes. Although ICGA suggested vascular involvement in previous studies, ICGA findings reported up to date are not specific for Behçet uveitis.[7–11] Therefore, use of ICGA has not been recommended on a routine basis in patients with Behçet uveitis.[2,3,10] The results of this study are in agreement with previous reports.

An important finding of this study was the occurrence of choroidal stromal expansion in eyes with active Behçet uveitis evidenced upon segmentation of the choroid into choroidal stroma and choroidal vessel lumen using custom software. Patients with Behçet uveitis had a significantly higher CS:CVL ratio when compared with control subjects. However, choroidal stromal expansion was not associated with thickening of the choroid, as we were not able to show any significant thickening of the subfoveal choroid in patients with an acute attack of Behçet uveitis. It has been suggested that inflammatory cells start to accumulate in the inner choroidal stroma because blood vessels in Sattler's layer have thinner walls compared with the larger vessels in Haller's layer.[39] We hypothesize that the choroidal inflammatory infiltration in patients with active Behçet uveitis apparent upon CS:CVL ratio analysis might be related to this fact. It has also been suggested that inflammatory conditions that primarily affect the inner choroid are less likely to cause thickening of the whole choroid.[40] Based on our results, we speculate that the inner choroidal vessels may be predominantly involved in Behçet disease. This may be of primary nature or secondary to the neighboring retinal inflammation.

To date, there is very limited information on segmentation of the choroid into stroma and vessel lumen on EDI OCT images. Branchini et al first calculated CS:CVL ratio in normal eyes using Otsu threshold and MATLAB software.[22] Kawano et al[41] segmented the choroid using Niblack threshold and imageJ software in eyes with Vogt-Koyanagi-Harada disease. The authors analyzed choroidal changes induced by high-dose systemic corticosteroid treatment. As expected, choroidal thickness was significantly reduced from 678.8 ± 150.2 μm at baseline to 363.3 ± 74.3 μm at 1 week and 307.8 ± 61.3 μm at 1 month. Luminal area-to-choroidal area ratio was 0.60 ± 0.03 at baseline, 0.67 ± 0.04 at 1 week, and 0.66 ± 0.04 at 1 month. There was a significant increase from the baseline at 1 week but not from 1 week to 1 month. This finding implies that there is massive stromal infiltration with compression of vessels and thickening of the choroid during the acute phase of Vogt-Koyanagi-Harada disease which responds favorably to therapy. Because massive inflammatory infiltration of the choroid occurs in patients with Vogt-Koyanagi-Harada disease, choroidal changes are striking, as opposed to patients with Behçet uveitis where no such robust changes occur in the choroid.

Our study group was biased by the inclusion of patients where imaging of the posterior segment could

be reliably performed. Patients with more severe vitreous haze and possibly more severe inflammation could have more robust changes in the choroid. Current technology does not allow investigation of such cases. High-speed image acquisition and deeper tissue penetration of the long-wavelength swept-source OCT technology results in better identification of the choroidoscleral interface and lower scattering attenuation in the retinal pigment epithelium and choroid.[42] Therefore, swept-source OCT may serve as a superior tool in revealing pathological changes in the choroid in patients with severe intraocular inflammation. We believe that advances in OCT angiography will also provide information on choroidal vascular alterations in Behçet uveitis.

In conclusion, we demonstrated that there was no significant change in the subfoveal choroidal thickness as measured by EDI OCT in a homogenous group of patients who had 4 years or less of disease duration, and had an acute posterior attack of Behçet uveitis. However, there was a significant change in the choroidal stroma-to-vessel lumen ratio which was not associated with a thickening in the subfoveal choroid. We assume that this might be related to inner stromal involvement in Behçet uveitis. Our results support the fact that FA remains the gold standard in monitoring inflammation in Behçet uveitis. Indocyanine green angiography was nonrewarding in assessing the extent of choroidal inflammation. Central foveal thickness may be used as a noninvasive measure to assess the inflammatory activity in patients with early Behçet uveitis.

Key words: Behçet uveitis, central foveal thickness, choroidal stroma, choroidal vessel lumen, enhanced depth imaging, fluorescein angiography, indocyanine green angiography, optical coherence tomography, subfoveal choroidal thickness.

References

1. Tugal-Tutkun I, Onal S, Altan-Yaycioglu R, et al. Uveitis in Behcet disease: an analysis of 880 patients. Am J Ophthalmol 2004;138:373–380.
2. Tugal-Tutkun I. Imaging in the diagnosis and management of Behcet disease. Int Ophthalmol Clin 2012;52:183–190.
3. Tugal-Tutkun I, Ozdal PC, Oray M, Onal S. Review for diagnostics of the year: multimodal imaging in Behçet uveitis. Ocul Immunol Inflamm 2017;25:7–19.
4. Charteris DG, Barton K, McCartney AC, Lightman SL. CD4+ lymphocyte involvement in ocular Behcet's disease. Autoimmunity 1992;12:201–206.
5. George RK, Chan CC, Whitcup SM, Nussenblatt RB. Ocular immunopathology of Behcet's disease. Surv Ophthalmol 1997; 42:157–162.
6. Mullaney J, Collum LM. Ocular vasculitis in Behcet's disease. A pathological and immunohistochemical study. Int Ophthalmol 1985;7:183–191.
7. Matsuo T, Sato Y, Shiraga F, et al. Choroidal abnormalities in Behçet disease observed by simultaneous indocyanine green and fluorescein angiography with scanning laser ophthalmoscopy. Ophthalmology 1999;106:295–300.
8. Klaeger A, Tran VT, Hiroz CA, et al. Indocyanine green angiography in Behcet's uveitis. Retina 2000;20:309–314.
9. Bozzoni-Pantaleoni F, Gharbiya M, Pirraglia MP, et al. Indocyanine green angiographic findings in Behcet disease. Retina 2001;21: 230–236.
10. Atmaca LS, Sonmez PA. Fluorescein and indocyanine green angiography findings in Behcet's disease. Br J Ophthalmol 2003;87:1466–1468.
11. Gedik S, Akova Y, Yilmaz G, Bozbeyoglu S. Indocyanine green and fundus fluorescein angiographic findings in patients with active ocular Behcet's disease. Ocul Immunol Inflamm 2005;13:51–58.
12. Yanik B, Conkbayir I, Berker N, et al. Doppler ultrasonography findings in ocular Behcet's disease. Clin Imaging 2006;30: 303–308.
13. Iaccarino G, Cennamo G, Forte R, Cennamo G. Evaluation of posterior pole with echography and optical coherence tomography in patients with Behcet's disease. Ophthalmologica 2009;223:250–255.
14. Spaide RF, Koizumi H, Pozzoni MC. Enhanced depth imaging spectral-domain optical coherence tomography. Am J Ophthalmol 2008;146:496–500.
15. Ishikawa S, Taguchi M, Muraoka T, et al. Changes in subfoveal choroidal thickness associated with uveitis activity in patients with Behcet's disease. Br J Ophthalmol 2014;98: 1508–1513.
16. Kim M, Kim H, Kwon HJ, et al. Choroidal thickness in Behcet's uveitis: an enhanced depth imaging-optical coherence tomography and its association with angiographic changes. Invest Ophthalmol Vis Sci 2013;54:6033–6039.
17. Ataş M, Yuvacı I, Demircan S, et al. Evaluation of the macular, peripapillary nerve fiber layer and choroid thickness changes in Behcet's disease with spectral-domain OCT. J Ophthalmol 2014;2014:865394.
18. Coskun E, Gurler B, Pehlivan Y, et al. Enhanced depth imaging optical coherence tomography findings in Behcet disease. Ocul Immunol Inflamm 2013;21:440–445.
19. Kaburaki T, Namba K, Sonoda KH, et al. Behcet's disease ocular attack score 24: evaluation of ocular disease activity before and after initiation of infliximab. Jpn J Ophthalmol 2014;58:120–130.
20. Jabs DA, Nussenblatt RB, Rosenbaum JT; Standardization of Uveitis Nomenclature Working Group. Standardization of uveitis nomenclature for reporting clinical data. Results of the First International Workshop. Am J Ophthalmol 2005;140:509–516.
21. Otsu N. A threshold selection method from gray-level histograms. IEEE Trans Syst Man Cybernetics 1979;9:62–66.
22. Branchini LA, Adhi M, Regatieri CV, et al. Analysis of choroidal morphologic features and vasculature in healthy eyes using spectral-domain optical coherence tomography. Ophthalmology 2013;120:1901–1908.
23. Tugal-Tutkun I, Herbort CP, Khairallah M; Angiography Scoring for Uveitis Working Group. Scoring of dual fluorescein and ICG inflammatory angiographic signs for the grading of posterior segment inflammation (dual fluorescein and ICG angiographic scoring system for uveitis). Int Ophthalmol 2010;30:539–552.
24. Tugal-Tutkun I, Herbort CP, Khairallah M, Mantovani A. Inter-observer agreement in scoring of dual fluorescein and ICG inflammatory angiographic signs for the grading of posterior segment inflammation. Ocul Immunol Inflamm 2010;18:385–389.

25. Kang HM, Lee SC. Long-term progression of retinal vasculitis in Behçet patients using a fluorescein angiography scoring system. Graefes Arch Clin Exp Ophthalmol 2014;252:1001–1008.
26. Moon SW, Kim BH, Park UC, Yu HG. Inter-observer variability in scoring ultra-wide-field fluorescein angiography in patients with Behcet retinal vasculitis. Ocul Immunol Inflamm 2016:1–9. Epub ahead of print.
27. Dancey C, Reidy J. Statistics Without Maths for Psychology: Using SPSS for Windows. London, United Kingdom: Prentice Hall; 2004.
28. Hosmer DW, Lemeshow S. Applied Logistic Regression. 2nd ed. New York, NY: Wiley; 2000.
29. Kaburaki T, Araki F, Takamoto M, et al. Best-corrected visual acuity and frequency of ocular attacks during the initial 10 years in patients with Behçet's disease. Graefes Arch Clin Exp Ophthalmol 2010;248:709–714.
30. Yu HG, Kim MJ, Oh FS. Fluorescein angiography and visual acuity in active uveitis with Behçet disease. Ocul Immunol Inflamm 2009;17:41–46.
31. Kaçmaz RO, Kempen JH, Newcomb C, et al; Systemic Immunosuppressive Therapy for Eye Diseases Cohort Study Group. Ocular inflammation in Behçet disease: incidence of ocular complications and of loss of visual acuity. Am J Ophthalmol 2008;146:828–836.
32. Demiroğlu H, Barişta I, Dündar S. Risk factor assessment and prognosis of eye involvement in Behcet's disease in Turkey. Ophthalmology 1997;104:701–705.
33. Novotny HR, Alvis D. A method of photographing fluorescence in circulating blood of the human eye. Tech Doc Rep SAMTDR USAF Sch Aerosp Med 1960;60-82:1–4.
34. Novotny HR, Alvis DL. A method of photographing fluorescence in circulating blood in the human retina. Circulation 1961;24:82–86.
35. Kogure K, Choromokos E. Infrared absorption angiography. J Appl Physiol 1969;26:154–157.
36. Yannuzzi LA, Slakter JS, Sorenson JA, et al. Digital indocyanine green videoangiography and choroidal neovascularization. Retina 1992;12:191–223.
37. Staurenghi G, Bottoni F, Giani A. Clinical applications of diagnostic indocyanine green angiography. In: Ryan SJ, Sadda SR, Hinton DR, eds. Retina. London, United Kingdom: Elsevier Saunders; 2013:51–81.
38. Takeuchi M, Iwasaki T, Kezuka T, et al. Functional and morphological changes in the eyes of Behçet's patients with uveitis. Acta Ophthalmol 2010;88:257–262.
39. Invernizzi A, Mapelli C, Viola F, et al. Choroidal granulomas visualized by enhanced depth imaging optical coherence tomography. Retina 2015;35:525–531.
40. Zarranz-Ventura J, Sim DA, Keane PA, et al. Characterization of punctate inner choroidopathy using enhanced depth imaging optical coherence tomography. Ophthalmology 2014;121:1790–1797.
41. Kawano H, Sonoda S, Yamashita T, et al. Relative changes in luminal and stromal areas of choroid determined by binarization of EDI-OCT images in eyes with Vogt-Koyanagi-Harada disease after treatment. Graefes Arch Clin Exp Ophthalmol 2016;254:421–426.
42. Adhi M, Liu JJ, Qavi AH, et al. Choroidal analysis in healthy eyes using swept-source optical coherence tomography compared to spectral domain optical coherence tomography. Am J Ophthalmol 2014;157:1272–1281.